Materials and Design 195 (2020) 109054

Contents lists available at ScienceDirect

Materials and Design

journal homepage: www.elsevier.com/locate/matdes

Templating effect of alginate and related biopolymers as hydration accelerators for calcium alumina cement - A mechanistic study

Alexander Engbert, Johann Plank *

Technische Universität München, Lichtenbergstr. 4, 85747 Garching, Germany

HIGHLIGHTS

- Proposed mechanism behind the accelerating effect of alginate on CAC hydration was assembled through in-depth investigation.
- Addition of alginate shortens the induction period of the hydration reaction which prompts earlier formation of C-A-H phases.
- Alginate sorbs high amount of Ca^{2+} as well as $[Al(OH)_4]^-$ ions, thus reducing concentration of free ions in pore solution.
- C-A-H phases form via deposition of Ca^{2+} / $[Al(OH)_4]^-$ onto the biopolymer, thereby generating a heterogeneous nucleation surface

GRAPHICAL ABSTRACT

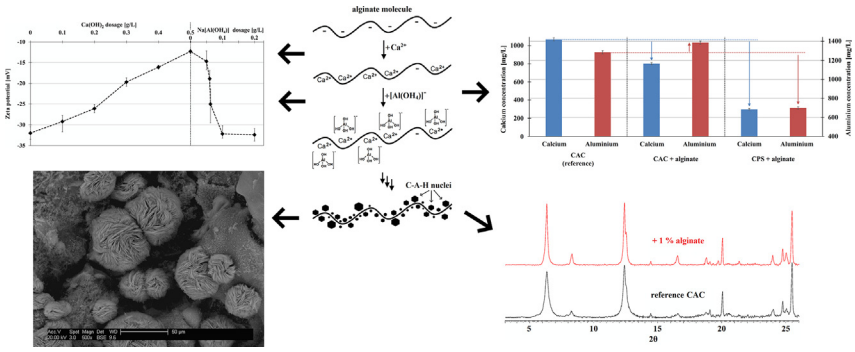

ARTICLE INFO

Article history:
Received 4 May 2020
Received in revised form 17 July 2020
Accepted 8 August 2020
Available online 10 August 2020

Keywords:
Biopolymer
Calcium aluminate cement
Hydration
Mechanism
Crystallization

ABSTRACT

In earlier publications it has been demonstrated that alginate and similarly structured biopolymers unexpectedly accelerate the hydration of calcium alumina cement. Here, this effect is investigated by applying ^{27}Al MAS NMR spectroscopy and XRD technique to track the hydration reaction and identify the hydration products. In the presence of these biopolymers an earlier consumption of clinker phases was observed indicating a shortened induction period. The subsequent formation of hydration products occurs earlier, resulting in the formation of C-A-H phases (CAH_{10} and C_2AH_8). No further reaction products like intercalation compounds were detected. An in-depth mechanistic study revealed that alginate does not adsorb on cement, but captures Ca^{2+} ions from the pore solution, thus resulting in a positively charged biopolymer chain which then attracts $[Al(OH)_4]^-$ ions to its surface. Through this binding of calcium and aluminate ions and alignment to the alginate molecule, a precursor for calcium aluminate hydrates is formed which acts as a nucleation seed and triggers continued growth into large C-A-H crystals, similar as in related biotemplating processes which are known for calcite or brushite formation.

1. Introduction

Previous studies [1,2] have reported the surprising accelerating effect of alginate or pectin on the hydration of calcium alumina cement (CAC). This effect solely occurs in CAC and was not observed for silicate- or sulfoaluminate-based binders (OPC, CSA). Alumina cements

Abbreviations: C=, CaO; A =, Al_2O_3; S =, SiO_2; H =, H_2O; F =, Fe_2O_3; T =, TiO_2; M =, MgO.

* Corresponding author at: Technische Universität München, Munich, Lichtenbergstr. 4, 85747 Garching bei München, Germany.
E-mail address: sekretariat@bauchemie.ch.tum.de (J. Plank).

https://doi.org/10.1016/j.matdes.2020.109054

are mainly composed of monocalcium aluminate which hydrates according to a dissolution and precipitation mechanism. There, C-A-H phases such as e.g. CAH_{10} ($CaAl_2(OH)_8(H_2O)_2 \cdot xH_2O$) and C_2AH_8 ($[Ca_2Al(OH)_6]^+[Al(OH)_4 \cdot xH_2O]^-$) are formed via homogeneous and heterogeneous nucleation. Hydration of the clinker at room temperature precedes as described by the following reaction equation, where the formation of CAH_{10} (predominately below 15 °C) and C_2AH_8 (starting at about 15 °C) as well as the conversion to the latter is shown:

$$CA + 10\,H \rightarrow CAH_{10}$$

$$2\,CAH_{10} \rightarrow C_2AH_8 + AH_3 + 9\,H$$

$$2\,CA + 11\,H \rightarrow C_2AH_8 + AH_3$$

Lithium salts (e.g. Li_2CO_3) are commonly applied to accelerate the reaction of CAC with water in order to achieve rapid strength development after casting, e.g. in self-levelling underlayments (SLU) and flooring compounds. The mechanism behind this specific effect of the Li^+ cation still is under discussion. It was first addressed by *Rodger and Double* [3] in 1984 and additional work was published by *Matusinovic* [4,5], *Damidot* [6] and more recently by *Goetz-Neunhoeffer* [7]. The latter presented that Li^+ ions accelerate the hydration of the aluminate phases (CA, $C_{12}A_7$ etc.) through six interconnected pathways: (1) increased dissolution of the clinker via an improved permeability of the blocking aluminium hydroxo hydrate layer; (2) formation of $[LiAl_2(OH)_6]_2^+$ $[(OH)_2 \cdot x\,H_2O]^{2-}$ layered double hydroxide (LDH) as seeding material which decreases the Gibbs free activation energy ΔG which needs to be overcome to form C_2AH_8 clusters of a size larger than the critical nucleus; (3) this increases the Ca^{2+} / Al^{3+} ratio in solution which thermodynamically promotes the formation of C_2AH_8; (4) Li^+ ions are continuously recycled for binding of Al^{3+} ions which (5) reduces the Al^{3+} concentration in solution and (6) further triggers continued the dissolution of clinker as a result of the decreased Al^{3+} content in solution. In a recent publication by *Manninger* et al. [8], however, the mechanism in step (4) which is crucial for the accelerating effect was questioned. The authors observed that in a CAC/calcite mixture, a decrease of the Li^+ concentration present in the cement pore solution was observed without replenishment.

In the case of alginate or pectin, a mechanism similar to that of Li salts would be quite unlikely. A first investigation into the mechanism revealed a strong calcium binding capability of the biopolymer, resulting in a reduction of the free calcium ion concentration in the pore solution [1]. Here, a link between the calcium binding capacity and the accelerating effectiveness was observed, whereat alginate came out on top [2]. Such a calcium binding effect normally is observed for retarding admixtures [9] and not for accelerators. To the best of our knowledge, no such calcium binding effect has been reported for accelerators so far. Obviously, a completely different mechanism as compared to that of Li^+ comes into play when biopolymers such as alginate or pectin are admixed to alumina cement. (Bio)polymers on the other hand were generally found to retard the hydration of CAC with the exemption of anionic polymers of high molecular weight, which possess a favourable structure to effectively complex calcium ions [1,2].

Alginate and pectin (see Fig. 1) are natural biopolymers produced by extraction from brown algae (*Phaeophyceae)* and *Citrus* / *Malus* fruits, respectively. Their structural characteristics are as follows: Alginates are copolymers comprised of guluronic (G) and mannuronic (M) acid, with an average molecular weight between 10,000 and 600,000 Da. The monosaccharide units (M and G) are linked in different sequences such as GM, GG and MM, this way producing different steric arrangements as illustrated in Fig. 1. Especially the GG blocks are vital for the ionotropic gelling effect observed in the presence of divalent cations like Ca^{2+}, as described by the 'egg box' model (Fig. 2) [10–12]. Commercial pectin is comprised of a linear

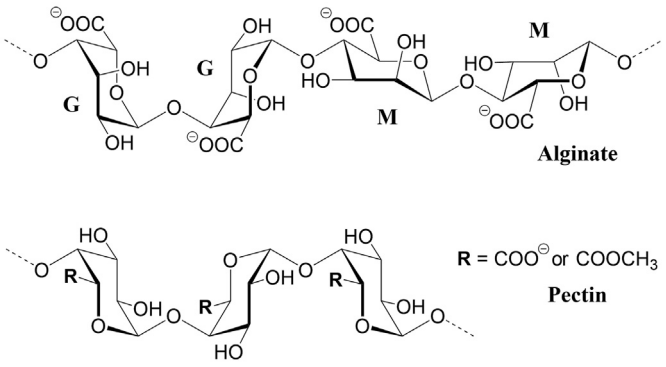

Fig. 1. Comparison of the molecular structures of alginate and pectin.

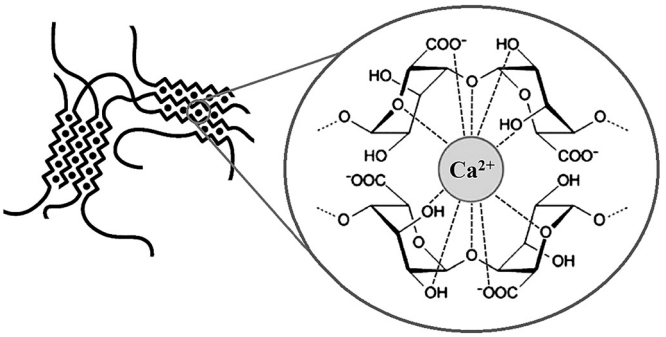

Fig. 2. Schematic representation of the Ca^{2+} induced complexation and gelation of alginate (adapted from [1]).

homopolymer of galacturonic acid (see Fig. 1) containing minor residues of rhamno galacturonan in the form of side chains composed of neutral sugars like arabinose and galactose. Pectins are distinguished by their degree of esterification (DE, ratio of methoxylate to carboxylate groups) and classified as high methoxylated (DE = 55–75%) or low methoxylated (DE = 20–45%) variant. The DE is crucial for its gelling properties. Only low methoxy pectin (LM pectin) gels in the presence of Ca^{2+} ions in a similar way as described by the "egg-box" model [10].

In the work presented here, mainly alginate was used in the investigations, because of its superior effectiveness. First, the impact of the polymer on the hydration of CAC was studied via ex-situ ^{27}Al MAS NMR spectroscopy and tracked the degree of hydration over time (0 −12h). Moreover, the formation of hydration products was monitored using ex-situ and in-situ XRD technique. Finally, the interaction of alginate with ions present in the pore solution (Ca^{2+} and $[Al(OH_4]^-$) was elucidated and based on those findings, a model for the working mechanism of accelerating biopolymers such as alginate was developed.

2. Experimental

2.1. Cement samples

Various calcium alumina cements containing different Al_2O_3 contents (*Ciment Fondu, Secar 51 and Secar 71,* supplied by *Imerys Aluminates, France)* were utilized in this study. Their mineralogical composition (Table 1) was analysed via XRD (*D8 advance* instrument, Bruker AXS, Karlsruhe, Germany) including *Rietveld* refinement (software *Topas 4.0*, Bruker AXS) and their oxide contents (values see [1]) were captured by XRF analysis (*Axios*, PANalytical, Kassel, Germany).

Table 1
Phase contents of the calcium alumina cement samples used in the study [1].

Phase	CAC sample (wt%)		
	Ciment Fondu	Secar 51	Secar 71
CA	47–57	64–74	54–64
CA_2	*n.d.*	*n.d.*	36–44
$C_{12}A_7$	1–5	< 1	< 1
C_4AF	10–20	*n.d.*	*n.d.*
C_2AS	1–10	18–22	< 1
C_2S	1–10	1–5	*n.d.*
Other	C_3FT, $C_{20}A_{13}M_3S_3$	CT, C_3FT	α-Al_2O_3 (< 2)

2.2. Materials

Deionised water was obtained from a *Barnstead Nanopore Diamond Water purification system* (*Werner Reinstwassersysteme*, Leverkusen, Germany) and was used in all experiments. Calcium hydroxide (*EMSURE*, > 99.7%) was procured from *Merck KGaA* (Darmstadt, Germany), while a sodium aluminate solution was prepared by reacting aluminium powder (1.35 g) in a sodium hydroxide (150 mL 1 M NaOH) solution followed by filtration.

2.2.1. Biopolymers

Two commercial biopolymer products, alginate sample *XEA 5036* (*Eurogum*) and pectin sample *CU 701* (*Herbstreith & Fox*), were utilized. Their characteristic properties are displayed in Table 2.

2.3. Experimental methods

2.3.1. Isothermal heat-flow calorimetry

Paste calorimetry was performed following DIN EN 196–11 [14] using sealable 10 mL glass ampoules. For testing, biopolymer powder was placed in the ampoule and dry-blended with four grams of cement. Deionised water was added to this blend and the paste was homogenised for two minutes via a vortex blender (*VWR*, Ismaning, Germany). The heat flow was monitored by placing the ampoules into an isothermal conduction calorimeter *TAM air model 3116–2* (*Thermometric*, Järfälla, Sweden) at 20 °C until heat evolution ceased.

2.3.2. Electrical conductivity

Following established methods [15,16], electrical conductivity of cement pastes was determined by using a self-built setup containing a *Qcond 2200* conductivity meter (*VWR International GmbH*, Germany). Here, the dissolution of the cement clinker phases as well as their interaction with admixtures can be observed via electrical conductivity which is linked to the amount of dissolved ions and species in the pore solution.

For this purpose, into a 5 L plastic beaker the cement (700 g of Secar 71), neat or dry-blended with e.g. 0.2 wt% alginate, was placed. Submerged into the cement powder were a stirrer (Eurostar KPG stirrer, *IKA-Werke*, Germany) with propeller shaped blades (4-leaf) and the conductivity probe. Then the stirrer was started, and water (490 g, w/c = 0.7) was added in one step. Conductivity values were recorded at ten-second intervals as soon as a homogeneous cement paste was obtained. Measurements were performed at 20 °C and recorded until the rate of conductivity increase dropped. Thereafter, values were taken at larger intervals, depending on the development of conductivity.

Table 2
Properties of the alginate and pectin samples used in the study.

Biopolymer	Product name	Properties
Sodium alginate	XEA 5036	M/G-ratio ≈ 0.8 [1]
LM-pectin	CU 701	M_w ≈ 320 kDa, M_n ≈ 63 kDa, GalA content ≈ 91%, DE ≈ 31% [13]

2.3.3. SEM imaging

SEM images were taken on a *XL–30 FEG* microscope (*FEI*, Eindhoven, Netherlands) using a secondary electron and backscattered electron detector. Magnifications ranged between 100× and 40,000×, and the accelerating voltage was between 4.0 kV and 30.0 kV. Samples were fixated on the sample holder stub with *Leit Adhesive Carbon Tabs* (*PLANO*, Wetzlar, Germany). After drying, the sample was sputtered with gold for improved conductivity. Alginate hydrogels were either dried through solvent exchange or freeze dried after gentle freezing with liquid N_2.

2.3.4. Zeta potential of cement pastes

The zeta potential of CAC paste was determined on a model *DT-300 Electroacoustic Spectrometer* (*Dispersion Technology Inc.*, Bedford Hills, New York). First, the ionic background of the cement pore solution was determined and subtracted from the zeta potential value obtained during titration of the biopolymer samples to the cement paste. To capture the dosage dependent zeta potential of CAC pastes, an aqueous alginate solution (0.25 wt%, pH = 7) was added stepwise (0.5 mL increments) to the cement slurry. The zeta potential of the cement paste was then recorded as a function of the biopolymer dosage.

2.3.5. Electrical charge of alginate

The electrical charge of alginate was determined in aqueous solution at 25 °C via laser Doppler micro-electrophoresis using a *Zetasizer* model *Nano ZS* (*Malvern Instruments*, UK). For this purpose, an alkaline alginate solution (0.15 wt% polymer; pH = 12, adjusted with NaOH) was investigated and the changes in the electrical charge of the polymer were monitored in dependence of the ionic composition of the polymer solution. Ascending concentrations of (1) calcium hydroxide or (2) the combination of an increasing concentration of sodium aluminate with a fixed amount of $Ca(OH)_2$ were added to the alginate solution and the zeta potential was determined for each system. For this purpose, in a centrifuge tube 10 mL samples were prepared by first placing 1 mL alginate solution (1.5 g/L). Then water was added, followed by the aluminate solution (0.9 g/L) and the calcium hydroxide solution (1.7 g/L). The sample was homogenised for approximately two minutes via shaking and placing in an ultrasonic bath (3 x 10s). Measurements were taken automatically after two minutes of thermal equilibration using a *Folded Capillary Zeta Cell*.

2.4. Analytical methods

2.4.1. Ion concentrations via ICP-OES

Inductively coupled plasma atomic emission (ICP-OES) spectrometry was conducted on a *series 700* instrument (*Agilent Technologies*, Santa Clara, CA, USA). The cement paste was prepared in a centrifuge tube by mixing e.g. 20 g Ciment Fondu dry-blended with 0.2 wt% biopolymer and subsequently homogenised for two minutes using a vortex mixer (*VWR*, Ismaning, Germany) after 10 mL of water had been added. The resulting paste was centrifuged (15 min at 8500 rpm) and the supernatant pore solution was filtrated via a membrane filter (0.2 μm PES). The solution was diluted at 1:30 (*v*/v) and the concentrations of Ca^{2+} and Al^{3+} in the pore solution were determined five times. Measurements were collected at several wavelengths and the resulting values were averaged. Deviation was calculated including an additional methodical error of 1% to account for inaccuracies resulting from e.g. pipetting and weighting.

2.4.2. X-ray diffraction

In-situ XRD was performed by placing the cement paste onto the sample holder and covering the paste with a *Kapton*® polyimide foil

(*VHG Labs*, Manchester, UK). Diffraction patterns were captured over 12 h every 30 min on a *D8 advance* instrument (*Bruker AXS*, Karlsruhe, Germany) equipped with a *VÅNTEC-1* detector (5–40° 2θ, 40 kV, 30 mA, 0.025° step, $t = 0.6$ s, fixed 0.5° divergence slit, *Bragg-Brentano* geometry and Cu Kα source). Because of the heat generated by the x-ray tube, the temperature in the chamber of the XRD rose to ≈ 27.5 °C during the in-situ measurements. Powder diffraction patterns were measured on the same *D8 advance* instrument (3–50° 2θ, 35 kV, 40 mA, 0.017° step, $t = 0.8$ s, variable divergence slit V6). Evaluation and processing of the diffraction patterns was performed using Bruker's *EVA V2* software.

2.4.3. ^{27}Al MAS NMR spectroscopy

Solid-state NMR experiments were performed on an *Advance 300* instrument (*Bruker BioSpin*, Karlsruhe, Germany) possessing a magnetic field strength of 7.0455 T and a ^{27}Al resonance frequency of 78.1 MHz. Chemical shifts were recorded relative to the external standard Al $(NO)_3 \cdot 9\,H_2O$.

Samples were prepared ex-situ by mixing cement, biopolymer and water in a centrifuge tube or a sealable glass ampule and subsequent storage at 20 °C for different periods of reaction time. Non-hardened samples were quenched with acetone and freeze-dried. Hardened samples were ground in a mortar and measured immediately. Samples were

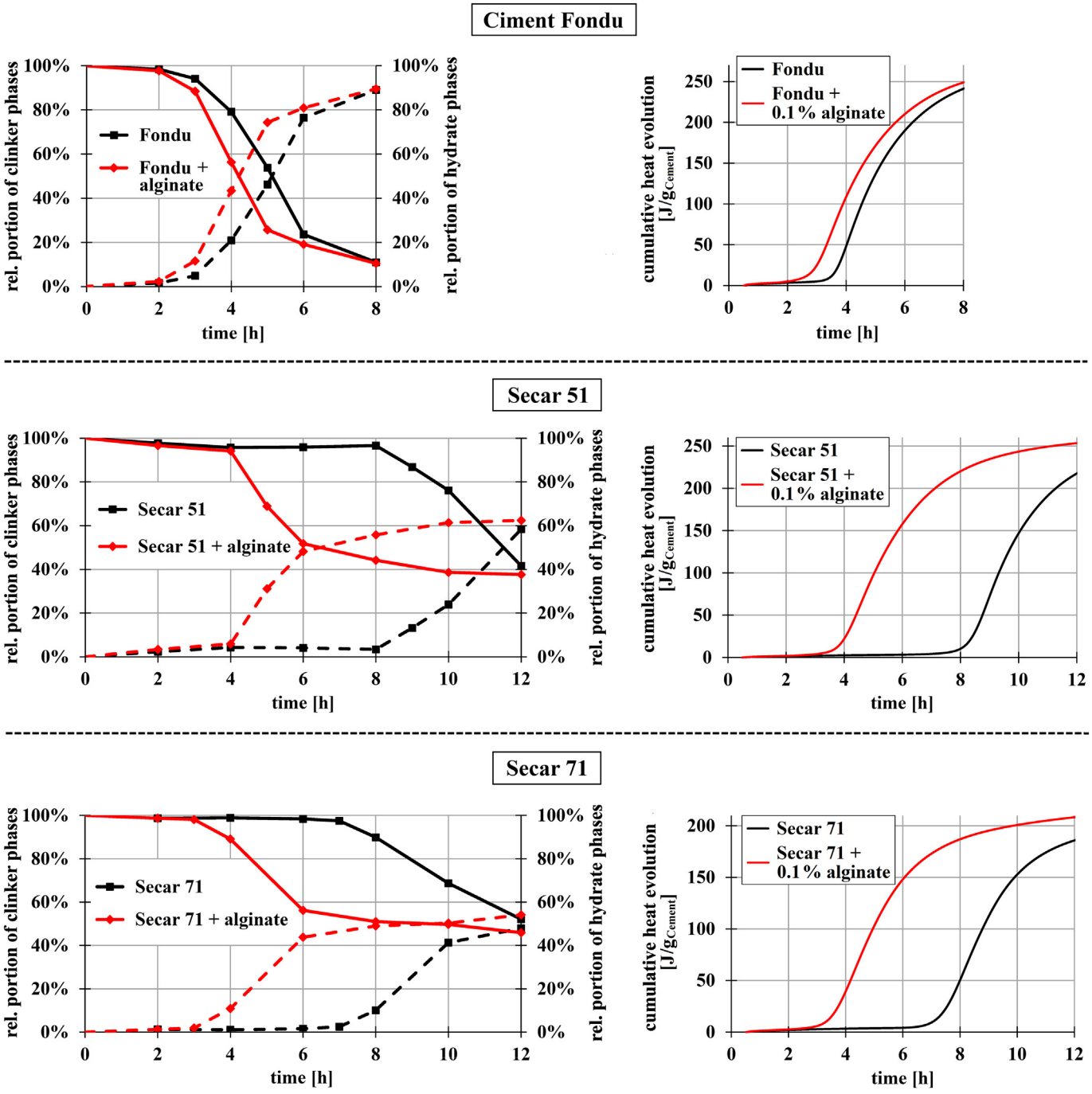

Fig. 3. Ex-situ ^{27}Al MAS NMR spectroscopic measurements (left) monitoring the time-dependent hydration of different CAC samples (w/b = 0.5) in the absence and presence of alginate (sample XEA 5036; bold line = clinker and dashed line = hydrate) and cumulative heat evolution of the corresponding samples (right).

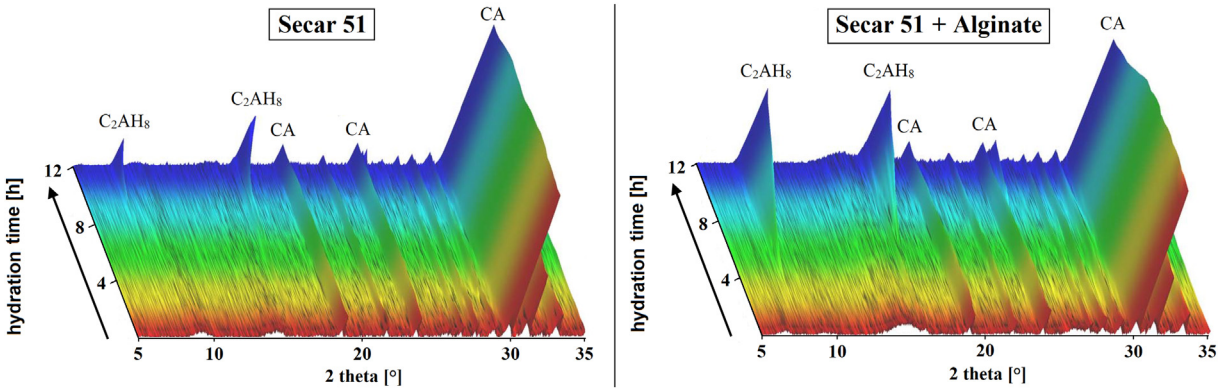

Fig. 4. In-situ XRD measurements monitoring the hydration of a CAC sample (Secar 51, w/b = 0.45, T ≈ 27.5 °C) over 12 h in the absence and presence of alginate sample XEA 5036.

filled into 4 mm zirconia rotors and rotated at 15 kHz. Single-pulse technique was used with a pulse width of 3 milliseconds. Repetition time was 2 s and the number of scans was 1000. Deconvolution and integration of the signals was performed after phase and background correction using *MNova 12* software (*Mestrelab Research*, Spain).

3. Results and discussion

Following the discovery of the accelerating effect of alginate and few other similarly structured polysaccharides [1,2], the working mechanism behind this unusual property still remained unclear. In order to investigate into this complex subject, at first the course of cement hydration was studied by tracking the time-dependent degree of the hydration and by analysing the hydration products formed. ^{27}Al MAS NMR spectroscopy was used to quantify the degree of hydration as a function of reaction time and ex-situ as well as in-situ XRD techniques were applied to identify the phases formed.

3.1. Tracking CAC hydration via ^{27}Al MAS NMR spectroscopy

The progress of hydration of an alumina cement can be quantified via ^{27}Al solid state NMR spectroscopy, as was reported by various authors before [e.g. 17]. The signals obtained from the clinker phases which contain tetrahedrally coordinated aluminium (Al-IV) and from the hydration products which contain octahedrally coordinated aluminium (Al-VI) can be integrated and express the degree of hydration of the cement. Here, the time dependent course of the hydration was studied ex-situ in cement pastes, neat as well as admixed with alginate (see exemplary NMR spectra for Secar 51 in Fig. S1 in supporting information). As cements, three mineralogically different CAC samples possessing Al_2O_3 contents between 45 and 70 wt% were utilized. According to the results exhibited in Fig. 3, two significant observations were made for all cements tested:

First, in the presence of alginate the induction period of CAC (represented by the portion of clinker which remained unreacted in the first hours after contact with water) is shortened as compared to the neat cement (black vs. red curve in Fig. 3, left). This effect is more pronounced in less reactive alumina cements with an increased Al_2O_3 content. Second, the observation of earlier hydration corresponds well with results obtained from heat flow calorimetry, as is shown in Fig. 3 (right). These observations are in accordance with literature reports for CAC hydration and comparable to the effect of lithium [17,18].

For example, in the paste holding Ciment Fondu within the first 8 h of hydration nearly all Al-IV reacts to Al-VI, whereas for the Secar 51 and Secar 71 pastes a consumption of only about 60% Al-IV is recorded over the first 12 h. This difference in hydration kinetics is caused by the different phase compositions of the cement samples. As such, Ciment Fondu which mainly contains CA and C_4AF (see Table 1) hydrates much faster than Secar 51 (main phases: CA and C_2AS) and Secar 71 (main phases: CA and CA_2) which hydrate slower because of their significant contents of gehlenite and grossite, respectively. At room temperature, gehlenite reacts only slowly over several weeks to form strätlingite [19], while it has been reported that grossite hydration begins only after the CA hydration decelerates [20]. Thus, the progress of hydration in the first 12 h for Secar 51 and Secar 71 is mainly dominated by the amount of CA contained in the clinker, and CACs holding higher

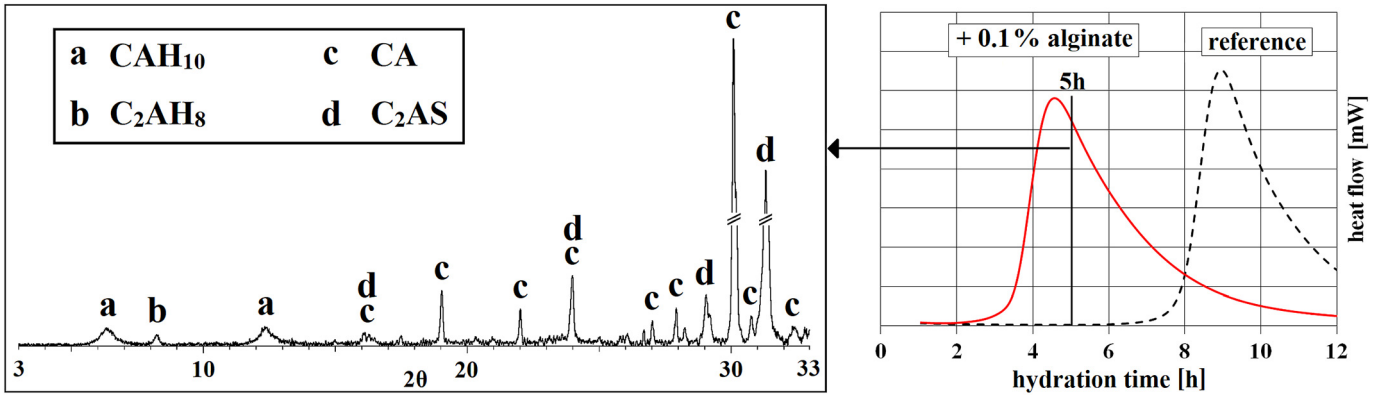

Fig. 5. X-Ray diffractogram (left) of ground CAC cement sample (Secar 51, w/b = 0.5) after five hours of hydration in the presence of 0.1 wt% alginate XEA 5036; and heat flow diagram (right) illustrating the time-dependent progress of hydration.

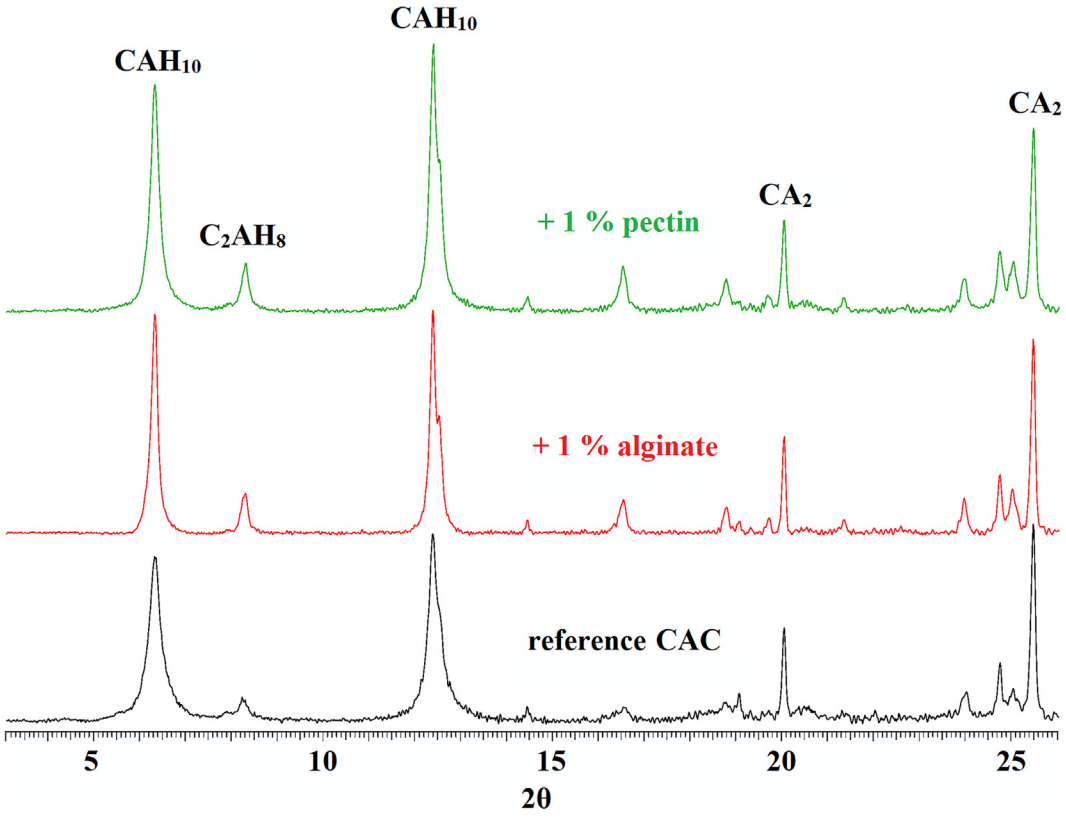

Fig. 6. XRD analysis of ground cement samples (Secar 71, w/b = 1, 20 °C) after 24 h of hydration in the absence or presence of 1 wt% alginate (sample XEA 5036) or pectin (sample CU 701).

amounts of this phase respond stronger to the alginate's accelerating effect.

3.2. Formation of hydrate phases tracked via XRD

Following the NMR investigation, hydration of the cement samples was also studied using X-ray diffraction in order to identify the specific hydrate phases (e.g. CAH_{10}, C_2AH_8, C_4AH_{13}, C_3AH_6) formed during the reaction with water.

First, in-situ XRD measurements were performed to monitor the time-dependent phase development of a Secar 51 sample in the absence and presence of alginate. There, it became obvious that in the presence of alginate, C_2AH_8 which presents the main hydration product of a CAC under those conditions, crystallizes earlier (shorter induction period) and thus in larger quantity (Fig. 4). The fact that only C_2AH_8 and no CAH_{10} was detected is explained in earlier literature [9]. According to these studies, when a transparent polymer foil (e.g. *Mylar* or *Kapton*) is used for in-situ measurements, as is the case here, then the water is retained in the sample which favours the formation of C_2AH_8. Furthermore, the formation of C_2AH_8 is also promoted by the increased temperature in the diffractometer under in-situ conditions. Because temperature influences the formation of hydrate phases thermodynamically, further ex-situ measurements of CAC hydrated at a definite temperature were conducted. Thus, for example at 10 °C only formation of CAH_{10} was detected.

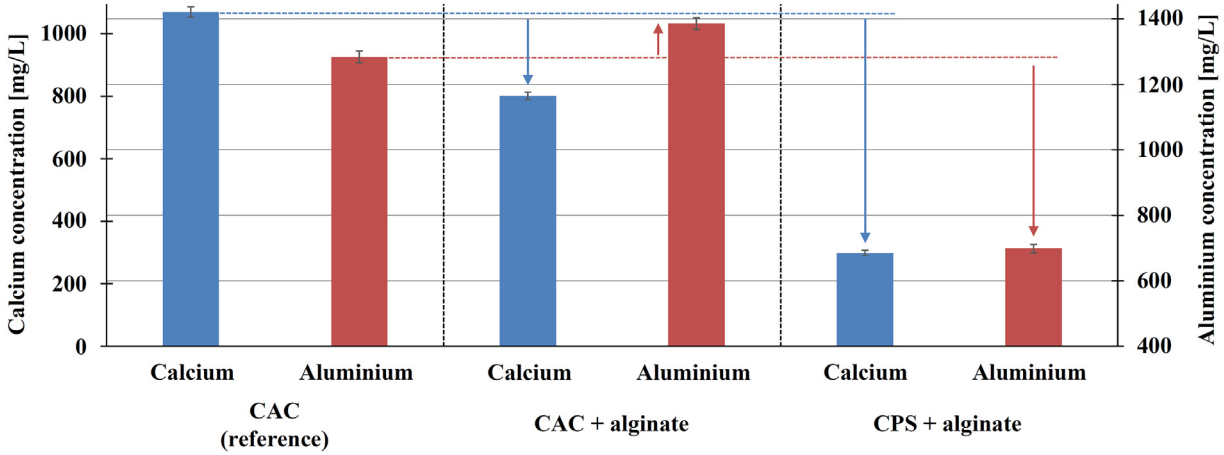

Fig. 7. Ca^{2+} and Al^{3+} ion concentrations in the pore solution (CPS) of Ciment Fondu (w/b = 0.5) after addition of 0.2 wt% alginate to the CAC paste or the CPS.

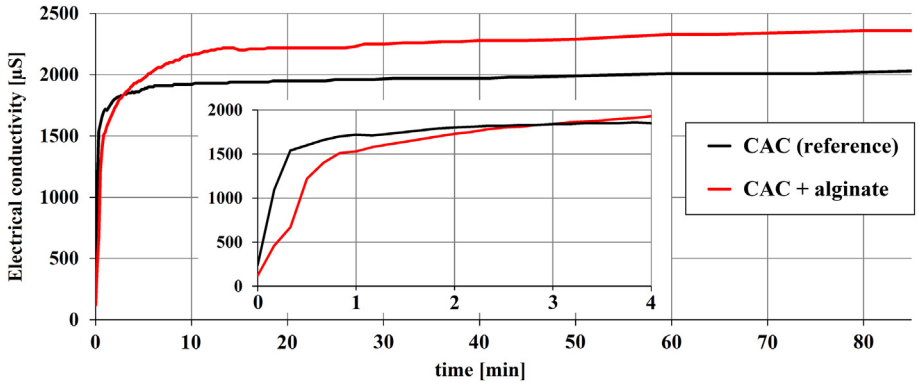

Fig. 8. Electrical conductivity of a CAC paste, neat and admixed with alginate (Secar 71, w/b = 0.7; 0.2 wt% alginate sample XEA 5036).

Furthermore, the early phase development after 5 h of hydration ($T = 20$ °C) was studied using powder XRD of a ground solidified sample (Fig. 5, left). Here, for the sample admixed with alginate, at the peak of the acceleration period the appearance of both C_2AH_8 as well as CAH_{10} was observed. Moreover, in accordance with the results from heat flow calorimetry (see Fig. 5, right) it was also noticed that after five hours of hydration the cement paste without alginate still was liquid while the paste containing the biopolymer already had stiffened and begun to harden. Apparently, alginate induces an earlier formation of C-A-H phases which results in an earlier strength development [1].

It is well established that hydrating alumina cement can chemically intercalate anionic polymers into the interlayer space of hydrates, thereby forming layered organo-mineral phases of the hydrocalumite type, abbreviated as Ca-Al-polymer-LDH [21]. These intercalation compounds are isostructural with the main hydration products of CAC (e.g. C_2AH_8) and therefore could act as a seeding and nucleation enhancing material and thus play a major role in the accelerating effect of the biopolymers. For this reason, their potential formation in the systems studied here was investigated.

The diffractograms presented above (Figs. 4 and 5) do not show any reflection at low 2θ angles (e.g. 2–5°) which are characteristic for such intercalation compounds [22]. However, considering the low addition rate of alginate in this experiment (0.1 wt%), the formation of such a by-product cannot be ruled out completely, because signal intensity for these organo-mineral phases might be too low. Thus, in order to clarify the potential formation of such Ca-Al-biopolymer LDHs, additional tests at significantly higher dosages of up to 1 wt% were performed by admixing either alginate or pectin to Secar 71. Even at such high additions, no occurrence of reflections characteristic for these intercalates was observed at 2θ angles <5°. As an example, the XRD diffractograms of the pastes holding 1 wt% of alginate or pectin are displayed in Fig. 6 (an overlap of the diffraction patterns is shown in Fig. S2 in the

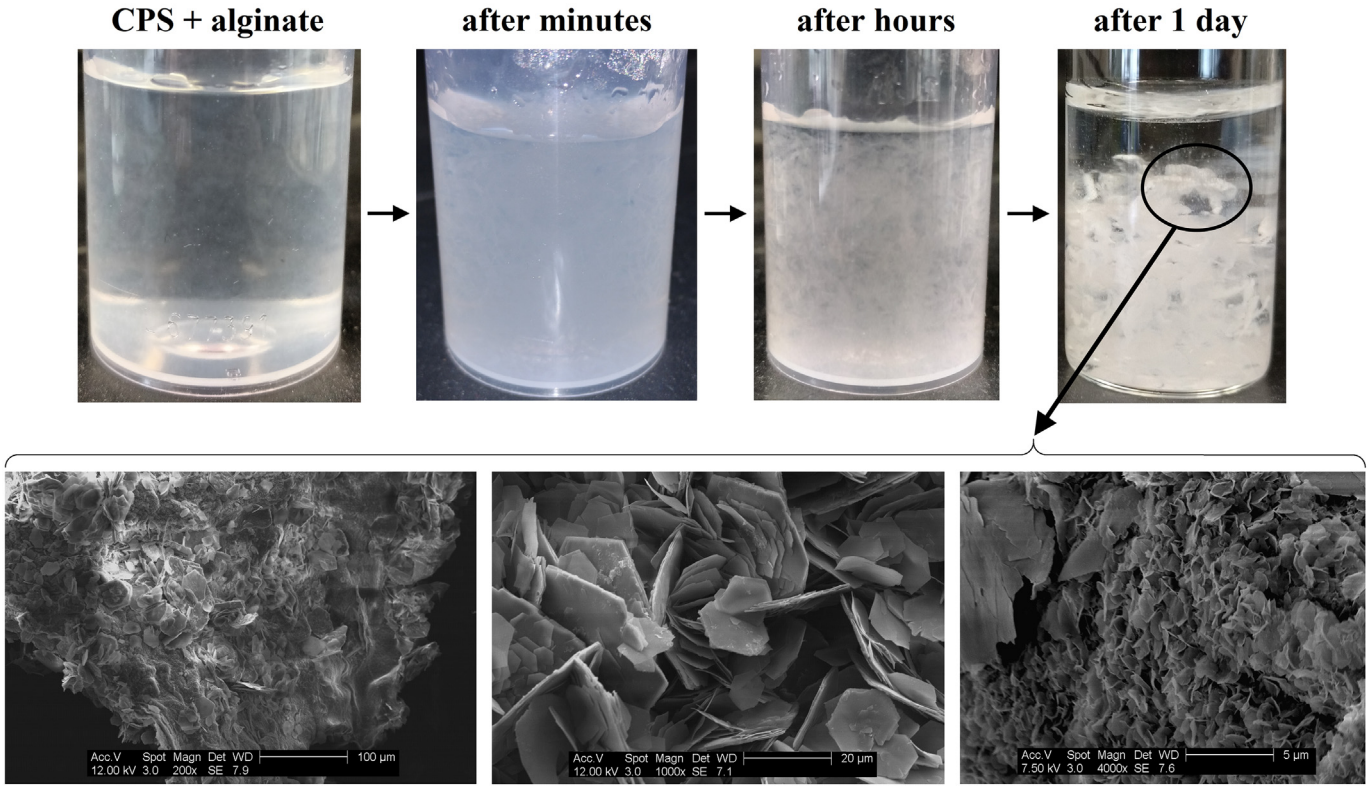

Fig. 9. Time-dependent behavior of alginate in CPS (top) and SEM images of the precipitated particles (bottom); magnifications (from left to right): 200×, 1000×, 4000×.

supplementary information). There, more intense peaks representing the hydrates C_2AH_8 and CAH_{10} were recorded when the biopolymers were present, thus confirming the accelerating effect of the polysaccharides.

Based upon these findings it can be concluded that different to the previously mentioned mechanism for Li-Al-LDH compounds [4–8], here the formation of biopolymer-containing Ca-Al-LDH intercalation compounds does not occur and hence plays no role in the accelerating effect of these polysaccharides. The absence of Ca-Al-biopolymer-LDHs can be explained with the strong interaction of these biopolymers with calcium ions in solution whereby after contact with Ca^{2+} the alginate molecule becomes much less anionic which significantly decreases its quality as guest molecule for intercalation into the LDH host structure.

To further study the interaction of the biopolymers with CAC the zeta potential of cement pastes which were stepwise admixed with alginates (sample XEA 5036 and a low M_w alginate, KIMICA ULV-L3 - properties see [1]) or pectin (sample CU 701) was measured. There, no change in the surface charge of the cement particles was detected, thus ruling out adsorption of the biopolymers on CAC. Thus, it can be assumed that the accelerating effect of the biopolymers only involves processes which occur in the pore solution and not on the surface of cement or its hydrates.

3.3. Interaction with ions in the pore solution

In the following, the interaction of alginate with Ca^{2+} and $[Al(OH)_4]^-$ ions present in the cement pore solution (pH ≈ 12) was investigated. At first, the ion concentrations in the pore solution of Ciment Fondu were determined. For this purpose, the cement was mixed for 2 min with water (w/c = 0.5), then centrifuged, filtered off and the resulting cement pore solution (CPS) was analysed for its content of Ca^{2+} and Al^{3+}, respectively using ICP-OES. As displayed in Fig. 7 (left), the initial concentration of Ca^{2+} was 1069 mg/L while Al^{3+} was present at 1284 mg/L in the CPS.

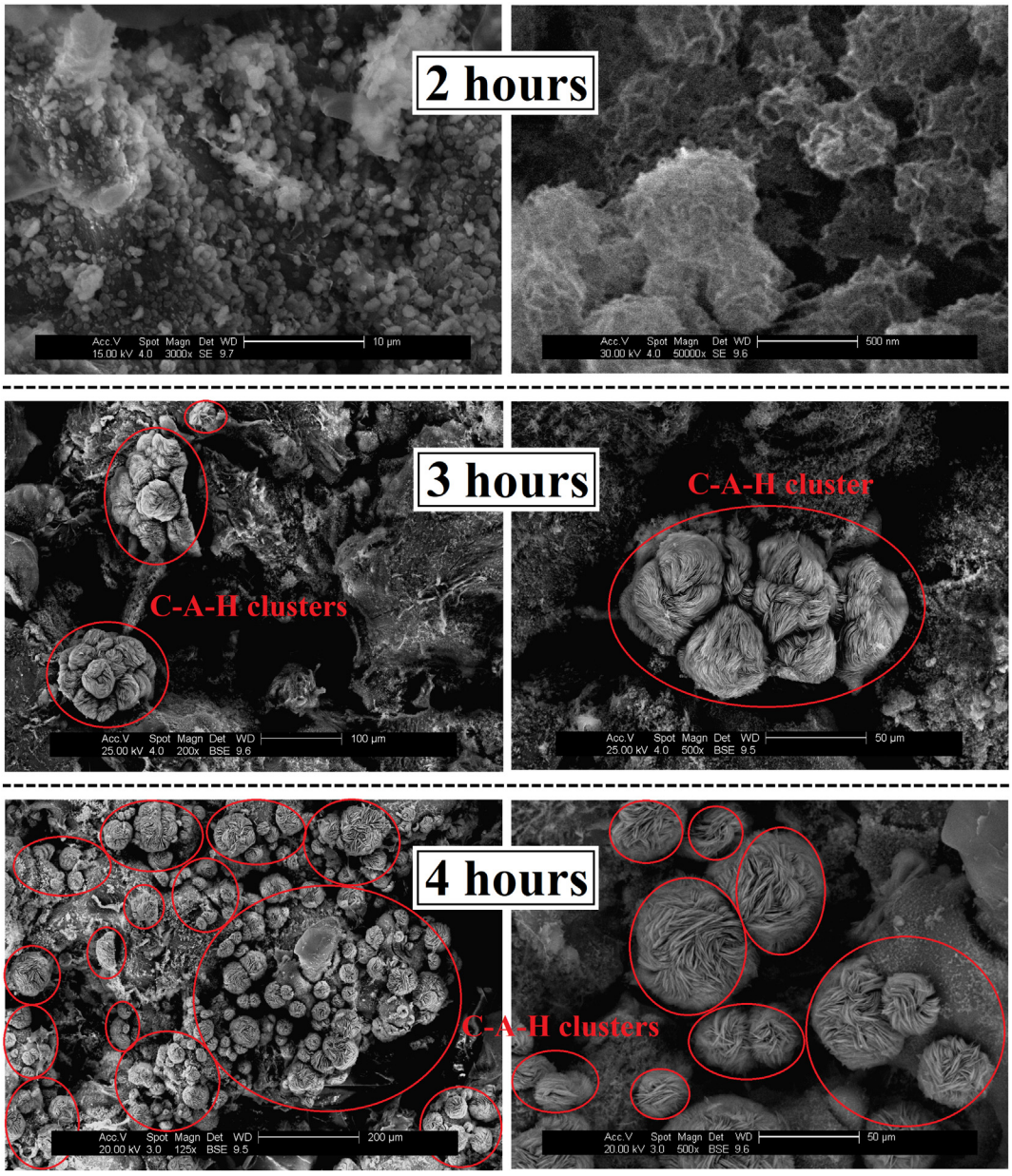

Fig. 10. Surfaces of freeze-dried alginate hydrogel submerged in CPS after various times of imbibition, as observed via SEM (magnification increasing from left to right).

To probe the impact of alginate on the ion concentrations, in the next step the same cement slurry was prepared, however 0.2 wt% of alginate were dry-blended into the cement. As can be seen from Fig. 7 (middle), in this case the concentration of Ca^{2+} is reduced from 1069 mg/L (in the neat paste) to 801 mg/L when the alginate is present. Contrary to this trend, the concentration of Al^{3+} increases from 1284 mg/L (for the neat paste) to 1386 mg/L in the presence of alginate. The same increase for Al^{3+} has been observed for Secar 51 and Secar 71 cement, respectively when alginate was admixed to them. There as well a reduction in the Ca^{2+} concentration and an increase in the Al^{3+} concentration was monitored.

The results can be interpreted as follows: alginate captures significant amounts of Ca^{2+} in its molecular cavity, as is well established and described by the 'egg-box' model [12]. As a consequence of the reduced Ca^{2+} concentration and stimulated by the solution equilibrium, more of the CA phase dissolves to replenish the Ca^{2+} which was taken up by the biopolymer. Consequently, the concentration of Al^{3+} rises above its initial value. The elevated aluminate concentrations could promote the formation of aluminate hydrates such as e.g. CAH_{10}. This mechanism of replenishment for Ca^{2+} could well explain why a polymer which captures Ca^{2+} can accelerate and not retard the hydration of CAC.

In order to confirm this model, a pore solution of neat Ciment Fondu was extracted and the CPS was treated with 0.2 wt% alginate (related to the mass of the cement), mixed for 2 min and after centrifugation and filtration was analysed for the ion contents. As is shown in Fig. 7 (right), there both the Ca^{2+} as well as the Al^{3+} concentrations drop significantly. Also, for Ca^{2+} the reduction is much more pronounced (from 1069 mg/L to 299 mg/L) than for Al^{3+} (1284 mg/L to 698 mg/L). This experiment confirms the preferred Ca^{2+} binding capacity of alginate, but also hints to an interaction of the biopolymer with the aluminate ion.

The latter was investigated further by mixing the same amount of alginate with a sodium aluminate solution of defined concentration (900 mg/L) and monitoring the Al^{3+} content, as it has been reported that in CPS sugars can form complexes with metal hydroxides [23–26]. Here, however, only a very minor decrease of ≈ 30 mg/L which is close to the margin of error was observed, thus indicating that a more complex mechanism is at work here.

These findings on the dissolution and complexing processes were further supported by conductivity measurements. Here, CAC pastes with and without alginate were continuously stirred and the electrical conductivity of the pore solution which directly correlates to the dissolved ions in the CPS was tracked. For this purpose, a CAC sample with 70% Al_2O_3 (Secar 71) was used because of its slower dissolution rate which allows for a better investigation of the early minutes of interaction with water and potentially alginate.

As displayed in Fig. 8, over the first three minutes alginate decreases the electrical conductivity, presumably as a result of the uptake of cations, especially Ca^{2+}, and the concomitant reduction in the charge of the biopolymer. However, thereafter this trend is reversed, and the conductivity of the paste admixed with alginate becomes higher than that of the neat paste, owed to increased clinker dissolution and the resulting higher aluminate concentration.

To conclude, the conductivity measurements support the previous finding from the pore solution analysis that alginate essentially triggers an increased dissolution of the clinker phases and especially increases

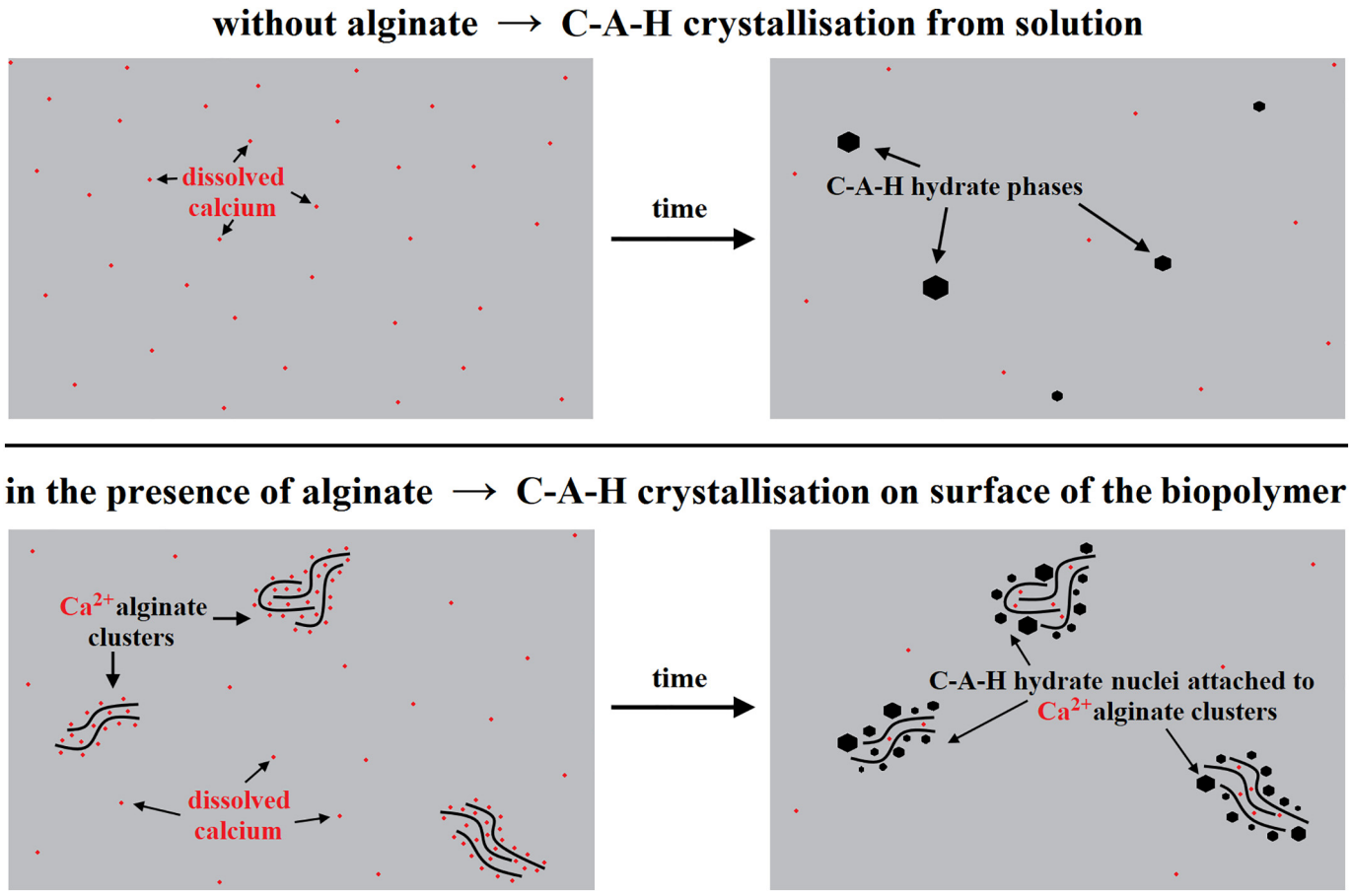

Scheme 1. Models for the C-A-H crystallization from neat CPS (top) and in the presence of alginate (bottom), where a templating effect involving the alignment of Ca^{2+} ions along the biopolymer chain takes place.

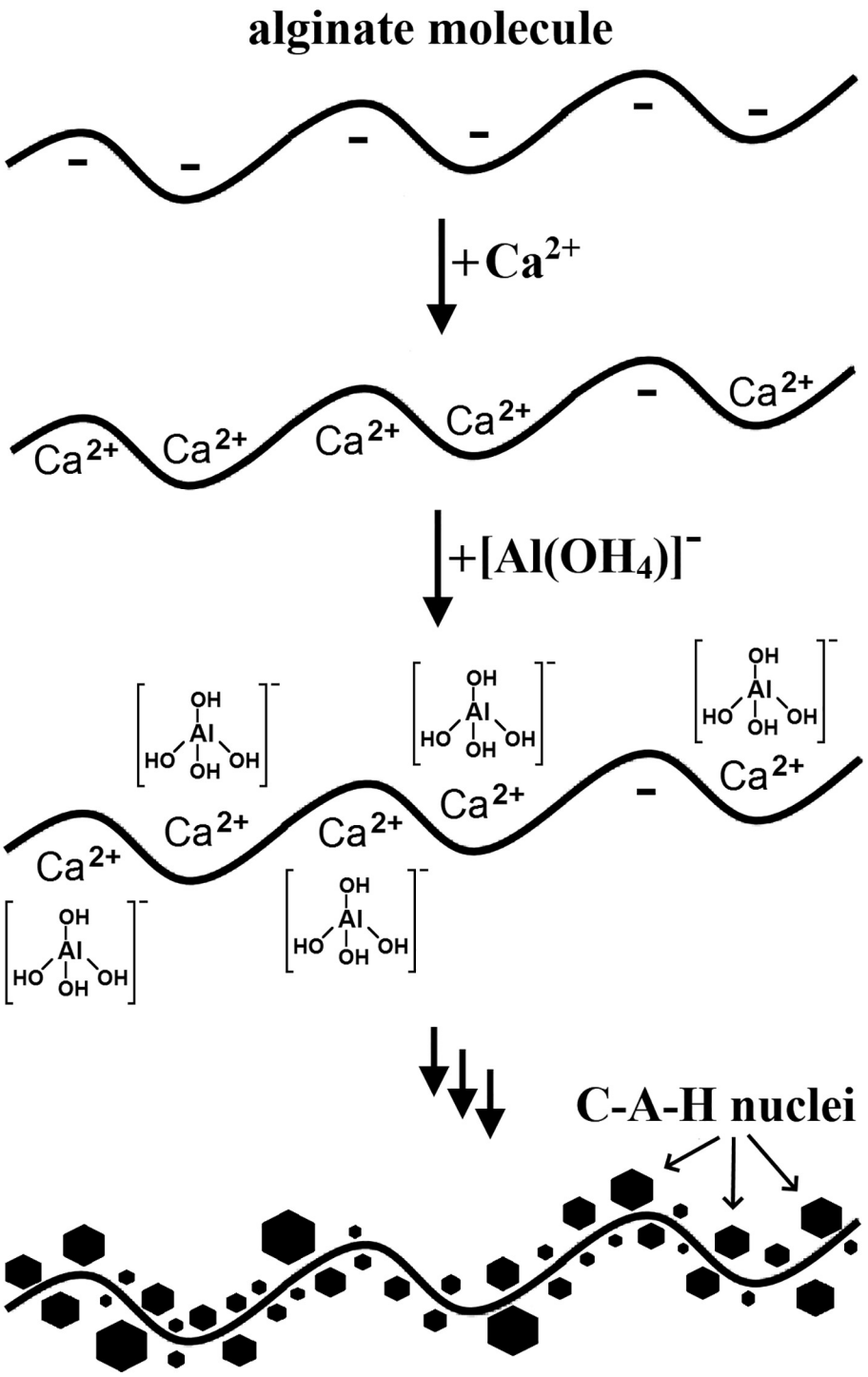

Scheme 2. Schematic illustration of the proposed interaction mechanism between alginate and Ca^{2+} as well as $[Al(OH)_4]^-$ ions in cement pore solution, leading to the formation of C-A-H phases.

the aluminate content in the resulting pore solution which might promote the precipitation of calcium aluminate hydrates, as observed in the XRD analysis before (see Figs. 4 and 5).

4. Proposed working mechanism for alginate

The investigations conducted so far can be summarized as follows:

- The accelerating effect is specific for alumina cements and differs with their reactivity which is dependent on their CA and $C_{12}A_7$ content. The more reactive a cement, the less effective is alginate [1].
- ^{27}Al solid state NMR spectroscopy and XRD confirm earlier formation of C-A-H phases and corresponding consumption of clinker phases in the presence of alginate (Figs. 3 and 4).
- Alginate does not intercalate or adsorb onto the surface of CAC or its hydrates. Hence, its accelerating effect derives from processes occurring in the pore solution.
- Alginate reduces the concentration of free Ca^{2+} in the pore solution through complexation via its 'cavity'. Furthermore, it also reduces

the amount of aluminate in solution (Fig. 7). Because aluminate ions cannot be chelated in the cavity like Ca^{2+}, it can be hypothesized that $[Al(OH)_4]^-$ ions coordinate with positively charged parts of the alginate resulting from Ca^{2+} uptake.

- Even in the presence of retarders such as e.g. citrate and tartrate, alginates still accelerate, in spite of significantly reduced concentrations of dissolved calcium and aluminate [1].

In consideration of this, still the question remains whether Ca^{2+} which has been captured by the alginate is irreversibly bound there or might be released to be incorporated into hydrate phases. Various literature reports (e.g. [27]) present that Ca^{2+} is in fact removed from the biopolymer when stronger chelators such as EDTA, sodium citrate or tartrate are added. Therefore, it can be assumed that at first calcium is extracted from the pore solution, but later is released to contribute to the formation of C-A-H phases. As such, by attracting and locally enriching Ca^{2+} ions along the molecule chain, alginate presents a heterogeneous crystallization surface, thus creating a reservoir and a template from which an initial cluster can nucleate and grow into a crystallite.

In order to verify the proposed mechanism, it was further studied whether C-A-H indeed crystallizes on the surface of the biopolymer chain. To investigate, at first a small amount of sodium alginate solution (2 wt%) was mixed with CPS (extracted from Ciment Fondu). Here, immediately upon addition formation of a slightly opaque hydrogel is observed, thus confirming abundant Ca^{2+} complexation. Furthermore, within a few hours the gel becomes increasingly cloudy and finally distinct particles precipitate from the solution (Fig. 9, top). This effect does not occur in Ca-alginate hydrogels, but only in CPS-alginate hydrogels, thus indicating that the combination of ions in CPS interact differently with alginate than individual Ca^{2+} or $[Al(OH)_4]^-$. Using SEM imaging the particles were identified as alginate polymer encrusted with platy C-A-H crystals (Fig. 9, bottom). Similar observations were also made for mixtures of pectin with CPS.

To further confirm this co-precipitation mechanism of alginate encrusted with C-A-H phases, alginate powder fixed to a sample holder or parts of a calcium alginate hydrogel were submerged in CPS and stored over up to four hours. For the alginate powder placed on the SEM sample holder, after 3 h the first C-A-H clusters were observed on the polymer surface, and after 4 h had covered most of the surface, as is displayed in Fig. 10.

Such templating effect of alginate, pectin and similarly structured biopolymers in biomineralization of e.g. $CaCO_3$ or brushite has been observed before by several authors [28–32]. For example, Ni-Al-LDH which is isostructural to several of the C-A-H phases can be prepared hydrothermally via a "facile biopolymer-assisted" crystallization process using alginate [33]. The proposed mechanism underlying this synthesis (Ni-Al-LDH nucleates and crystallizes along the alginate molecule) follows a similar pattern as the working mechanism which was proposed above for the accelerating effect of alginate on CAC hydration: In the following scheme, the templating effect which triggers C-A-H nucleation via initial interaction of alginate with Ca^{2+} ions is illustrated (Scheme 1). Thus, the proposed mechanism for the behavior of alginate in cement pore solution is supported by processes already known from comparable bio-based systems.

Still, this model does not yet explain the role of aluminate ions which when alginate is present in CPS also significantly decreases in concentration (see Fig. 7). We assume its behavior as follows: the interaction of Ca^{2+} with alginate results in a biopolymer chain exhibiting positive charges along its backbone (Scheme 2). To these sites, negatively charged $[Al(OH)_4]^-$ is attracted. Other authors have reported that while in aqueous solution alginate exhibits a negative electrical charge / zeta potential. In the presence of cations like Ca^{2+} or of cationic polymers (e.g. chitosan), the charge decreases and approaches zero [34,35]. Furthermore, it was found that in case of a layer-by-layer deposition of anionic alginate and cationic chitosan onto a planar surface, a charge reversal occurs with each additional layer ($Algi^- \rightarrow Chit^+ \rightarrow Algi^- \ldots$) [36].

In order to verify that a similar layer-by-layer deposition mechanism is at work here, the zeta potential of alginate in the presence of increasing dosages of calcium ions was determined. Here, the initially highly negative electrical charge of alginate was found to decrease from −32 mV to −12 mV (Fig. 11), similar as has been reported by [34,35], thus confirming the chelation of Ca^{2+} cations by the polysaccharide chain. Next, an increasing dosage of aluminate ions was fed into the alginate solution in combination with a fixed amount (0.5 g/L) of $Ca(OH)_2$. Interestingly, in the presence of $[Al(OH)_4]^-$ the trend for the charge reversed, and with increasing $Na[Al(OH)_4]$ concentration the zeta potential became more negative (from −12 mV to −32 mV, see Fig. 11). This observation confirms our concept that at first Ca^{2+} and in a second step $[Al(OH)_4]^-$ is attracted to the alginate molecule and coordinate to the biopolymer chain whereby at the high pH Ca-Al-OH clusters form which through continued uptake of Ca^{2+} and $[Al(OH)_4]^-$ ions from the pore solution grow into critical clusters and ultimately form the characteristic large, platy crystals of C-A-H phases (Scheme 2).

This mechanistic model combines all previous findings and can well explain why the accelerating effect (1) is absolutely specific for biopolymers possessing high Ca^{2+} capturing capability and (2) why this mechanism cannot work in OPC which does form C-A-H phases during its hydration.

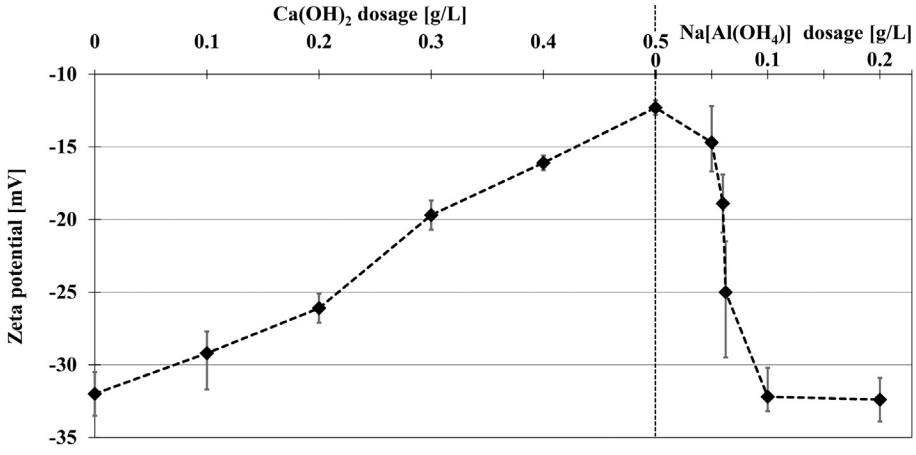

Fig. 11. Zeta potential of aqueous alginate solution (0.15 wt%, pH >12) as a function of increasing Ca^{2+} concentration (left) and $Na[Al(OH)_4]$ addition (right).

5. Conclusion

This study investigated the mechanism underlying the unexpected accelerating effect of alginates and similarly structured biopolymers on alumina cements by first using ^{27}Al MAS NMR spectroscopy to determine the degree of hydration and, second, XRD analysis to monitor hydrate phase development. From these experiments a shortening of the induction period during CAC hydration was evidenced via an earlier commencement of clinker dissolution. Obviously, in the presence of alginate the formation of hydrate phases starts earlier. Such promotion of C-A-H formation leads to an earlier strength development [1].

In order to elucidate the working mechanism which is responsible for this accelerating effect, the interaction between alginate and the ions present in the CAC pore solution was studied. Here, not only a strong complexation of calcium ions through the carboxylate groups in the 'cavity' of the biopolymer, but also an interaction with aluminate ions was found. These results suggested that a bi-layer is formed along the biopolymer chain whereby initially Ca^{2+} ions are captured by the alginate and subsequently aluminate anions are then aligned along the molecule chain, thus templating the essential constitutional part in calcium aluminate hydrates, the Ca-Al-OH building block, and triggering their nucleation and subsequent growth.

Based upon these finding a model is proposed for the mode of action of alginate as an accelerator in CAC. According to this, in CPS the alginate molecule provides a heterogeneous crystallization surface by generating favourable conditions for the very first nucleation and growth of C-A-H phases. This biotemplated process was substantiated by SEM images confirming the earlier nucleation and growth of C-A-H crystals on the surface of the biopolymer.

Currently, lithium salts such as Li_2CO_3 present the only viable accelerator for CAC. Due to the increased demand for lithium ion batteries in electromobility and the relatively limited availability of this element, the substitution of lithium salts in CAC applications appears to be highly urgent and almost compulsory. Biopolymers such as alginate or pectin which present green and renewable materials seem to offer an attractive alternative to replace the precious lithium compounds in calcium aluminate cements.

Declaration of Competing Interest

Funding was provided by Deutsche Forschungsgemeinschaft, Germany (DFG) under the grant PL-472/13-1 ("*Investigation on the replacement of lithium carbonate as accelerator for calcium aluminate cements and its underlying working mechanism*").

The authors wish to declare that no conflicts of interest or competing interests exists.

Acknowledgement

The authors are most grateful to *Imerys Aluminates* (formerly *Kerneos*) for the generous supply of aluminate cement samples. Especially Mr. A. Eisenreich and Dr. R. Kwasny-Echterhagen are thanked for their support. Our gratitude also goes to *Eurogum* and *Herbstreith & Fox* for providing the biopolymer samples. Moreover, the authors are most grateful to Deutsche Forschungsgemeinschaft, Bonn, Germany (DFG) for financing this project under the grant PL-472/13-1 ("*Investigation on the replacement of lithium carbonate as accelerator for calcium aluminate cements and its underlying working mechanism*"). Finally, the support of T. Burger (Chair for Technical Chemistry, TUM) for conducting the ICP-OES measurements is also acknowledged.

Appendix A. Supplementary data

Supplementary data to this article can be found online at https://doi.org/10.1016/j.matdes.2020.109054.

References

[1] A. Engbert, S. Gruber, J. Plank, The effect of alginates on the hydration of calcium aluminate cement, Carbohydr. Polym. 236 (2020) 116038.
[2] A. Engbert, J. Plank, Identification of specific structural motifs in biopolymers that effectively accelerate calcium alumina cement, Ind. Eng. Chem. Res. 59 (26) (2020) 11930–11939.
[3] S.A. Rodger, D.D. Double, The chemistry of hydration of high alumina cement in the presence of accelerating and retarding admixtures, Cem. Concr. Res. 14 (1) (1984) 73–82.
[4] T. Matusinović, D. Čurlin, Lithium salts as set accelerators for high alumina cement, Cem. Concr. Res. 23 (4) (1993) 885–895.
[5] T. Matusinovic, N. Vrbos, D. Čurlin, Lithium salts in rapid setting high-alumina cement materials, Ind. Eng. Chem. Res. 33 (11) (1994) 2795–2800.
[6] D. Damidot, A. Rettel, A. Capmas, Action of admixtures on Fondu cement: part 1 Lithium and sodium salts compared, Adv. Cem. Res. 8 (31) (1996) 111–119.
[7] F. Goetz-Neunhoeffer, Kinetics of the hydration of calcium aluminate cement with additives, ZKG Int. 58 (4) (2005) 65–72.
[8] T. Manninger, D. Jansen, J. Neubauer, F. Goetz-Neunhoeffer, Accelerating effect of Li_2CO_3 on formation of monocarbonate and Al-hydroxide in a CA-cement and calcite mix during early hydration, Cem. Concr. Res. 126 (2019) 105897.
[9] J. Bensted, Calcium aluminate cements, Structure and Performance of Cements, Second editionCRC Press, Boca Raton, USA 2002, pp. 114–138.
[10] A.P. Imeson, Food stabilisers, thickeners and gelling agents, Wiley Blackwell, Hoboken - New Jersey, USA, 2011.
[11] J. Plank, Applications of biopolymers in construction engineering, Biopolymers: Vol. 10 General Aspects and Special Applications, Wiley-VCH, Weinheim, Germany 2003, pp. 29–95.
[12] G.T. Grant, E.R. Morris, D.A. Rees, P.J. Smith, D. Thom, Biological interactions between polysaccharides and divalent cations: the egg-box model, FEBS Lett. 32 (1) (1973) 195–198.
[13] M.F. Borisenkov, A.P. Karmanov, L.S. Kocheva, et al., Adsorption of β-glucuronidase and estrogens on pectin/lignin hydrogel particles, Int. J. Polym. Mater. Polym. Biomater. 65 (9) (2016) 433–441.
[14] DIN EN 196--11, Methods of testing cement – part 11: heat of hydration – isothermal conduction Calorimetry method, German Version EN (2019) (196–11).
[15] A. Bier, A. Mathieu, B. Espinosa, J.P. Bayoux, Technical Paper 1: The Use of Conductimetry to Characterize the Reactivity of High Alumina Cements, Kerneos, France, 1993.
[16] C.D. Parr, C. Revais, H. Fryda, Technical Paper 18: The Nature of Chemical Reactions that Occur during Castable Installation and Analytical Techniques Used to Follow these Reactions, Kerneos, France, 1999.
[17] X. Cong, R.J. Kirkpatrick, Hydration of calcium aluminate cements: a solid state ^{27}Al NMR study, J. Am. Ceram. Soc. 76 (2) (1993) 409–416.
[18] T. Luong, H. Mayer, H. Eckert, T.I. Novinson, In situ ^{27}Al NMR studies of cement hydration: the effect of lithium-containing setting accelerators, J. Am. Ceram. Soc. 72 (11) (1989) 2136–2141.
[19] C. Gosselin, Microstructural Development of Calcium Aluminate Cement Based Systems With and Without Supplementary Cementitious Materials, Ph.D. thesis École Polytechnique Fédérale de Lausanne, Switzerland, 2009.
[20] S.R. Klaus, J. Neubauer, F. Goetz-Neunhoeffer, Hydration kinetics of CA_2 and CA - investigations performed on a synthetic calcium aluminate cement, Cem. Concr. Res. 43 (2013) 62–69.
[21] S. Ng, E. Metwalli, P. Müller-Buschbaum, J. Plank, Occurrence of intercalation of PCE superplasticizers in calcium aluminate cement under actual application conditions, as evidenced by SAXS analysis, Cem. Concr. Res. 54 (2013) 191–198.
[22] J. Plank, Z. Dai, N. Zouaoui, Novel hybrid materials obtained by intercalation of organic comb polymers into Ca–Al–LDH, J. Phys. Chem. Solids 69 (5–6) (2008) 1048–1051.
[23] J.F. Young, A review of the mechanisms of set-retardation in Portland cement pastes containing organic admixtures, Cem. Concr. Res. 2 (4) (1972) 415–433.
[24] T. dos Santos, C.I. Pereira, R. Gonçalves, et al., Gluconate action in the hydration of calcium aluminate cements: theoretical study, processing of aqueous suspensions and hydration reactivation, J. Eur. Ceram. Soc. 39 (8) (2019) 2748–2759.
[25] A. Pallagi, Interaction of Calcium With Sugar Type Ligands in Solutions Related to the Bayer Process, Ph.D. thesis University of Szeged, Hungary, 2012.
[26] F.R. Venema, J.A. Peters, H. Van Bekkum, Multinuclear magnetic resonance study of the coordination of aluminium (III) aldarate complexes with calcium (II) in aqueous solution, Recueil des Travaux Chimiques des Pays Bas 112 (7–8) (1993) 445–450.
[27] M. Kobašlija, D.T. McQuade, Removable colored coatings based on calcium alginate hydrogels, Biomacromolecules 7 (8) (2006) 2357–2361.
[28] M. Díaz-Dosque, P. Aranda, M. Darder, et al., Use of biopolymers as oriented supports for the stabilization of different polymorphs of biomineralized calcium carbonate with complex shape, J. Cryst. Growth 310 (24) (2008) 5331–5340.
[29] R. Fried, Y. Mastai, The effect of sulfated polysaccharides on the crystallization of calcite superstructures, J. Cryst. Growth 338 (1) (2012) 147–151.
[30] M.F. Butler, W.J. Frith, C. Rawlins, et al., Hollow calcium carbonate microsphere formation in the presence of biopolymers and additives, Crystal Growth Des. 9 (1) (2008) 534–545.
[31] S. Ucar, S.H. Bjørnøy, D.C. Bassett, et al., Nucleation and growth of Brushite in the presence of alginate, Cryst. Growth Des. 15 (11) (2015) 5397–5405.
[32] Z. Schnepp, Biopolymers as a flexible resource for nanochemistry, Angew. Chem. Int. Ed. 52 (4) (2013) 1096–1108.

[33] H. Wang, G. Fan, C. Zheng, et al., Facile sodium alginate assisted assembly of Ni—Al layered double hydroxide nanostructures, Ind. Eng. Chem. Res. 49 (6) (2010) 2759–2767.
[34] M. Cegnar, J. Kerč, Self-assembled polyelectrolyte Nanocomplexes of alginate, chitosan and ovalbumin, Acta Chim. Slov. 57 (2) (2010).
[35] L. Miao, C. Wang, J. Hou, et al., Effect of alginate on the aggregation kinetics of copper oxide nanoparticles (CuO NPs): bridging interaction and heteroaggregation induced by Ca^{2+}, Environ. Sci. Pollut. Res. 23 (12) (2016) 11611–11619.
[36] A. Acevedo-Fani, L. Salvia-Trujillo, R. Soliva-Fortuny, O. Martín-Belloso, Layer-by-layer assembly of food-grade alginate/chitosan nanolaminates: formation and physicochemical characterization, Food Biophys. 12 (3) (2017) 299–308.